

The melting points, yields, purities, and IR data of the 36 flavone derivatives

2-(2-fluorophenyl)-3-hydroxy-4*H*-chromen-4-one (**1**)

Yield: 56%; m.p. 150-156°C; purity: 98%; IR (ν/cm^{-1}) ν (C=O, conjugated) : 1606, ν (OH) : 3298

2-(2-fluorophenyl)-3-hydroxy-6-nitro-4*H*-chromen-4-one (**2**)

Yield: 96%; m.p. 194-200°C; purity: 98%; IR (ν/cm^{-1}) ν (C=O, conjugated) : 1622, ν (OH) : 3289

2-(4-fluorophenyl)-3-hydroxy-6-nitro-4*H*-chromen-4-one (**3**)

Yield: 33%; m.p. 240-244°C; purity: 96%; IR (ν/cm^{-1}) ν (C=O, conjugated) : 1612, ν (OH) : 3284

3-hydroxy-2-(4-methoxyphenyl)-4*H*-chromen-4-one (**4**)

Yield: 60%; m.p. 234-238°C; purity: 98%; IR (ν/cm^{-1}) ν (C=O, conjugated) : 1602, ν (OH) : 3189

3-hydroxy-2-(2-methoxyphenyl)-4*H*-chromen-4-one (**5**)

Yield: 62%; m.p. 210-212°C; purity: 98%; IR (ν/cm^{-1}) ν (C=O, conjugated) : 1607, ν (OH) : 3286

2-(3,4-dimethoxyphenyl)-3-hydroxy-4*H*-chromen-4-one (**6**)

Yield: 57%; m.p. 200-202°C; purity: 98%; IR (ν/cm^{-1}) ν (C=O, conjugated) : 1610, ν (OH) : 3211

3-hydroxy-2-(2,4,6-trimethoxyphenyl)-4*H*-chromen-4-one (**7**)

Yield: 62%; m.p. 190-194°C; purity: 98%; IR (ν/cm^{-1}) ν (C=O, conjugated) : 1605, ν (OH) : 3191

2-(2,4-dimethoxyphenyl)-3-hydroxy-4*H*-chromen-4-one (**8**)

Yield: 64%; m.p. 198-200°C; purity: 97%; IR (ν/cm^{-1}) ν (C=O, conjugated) : 1609, ν (OH) : 3306

2-(6-(4-methoxystyryl)-2,4-dimethoxyphenyl)-3-hydroxy-4*H*-chromen-4-one (**9**)

Yield: 46%; m.p. 206-210°C; purity: 98%; IR (ν/cm^{-1}) ν (C=O, conjugated) : 1610, ν (OH) : 3314

2-(6-(4-methoxystyryl)-2,4-dimethoxyphenyl)-3-hydroxy-6-nitro-4*H*-chromen-4-one (**10**)

Yield: 78%; m.p. 118-122°C; purity: 97%; IR (ν/cm^{-1}) ν (C=O, conjugated) : 1620, ν (OH) : 3323

2-(6-(4-methoxystyryl)-2,4-dimethoxyphenyl)-6-bromo-3-hydroxy-4*H*-chromen-4-one (**11**)

Yield: 71%; m.p. 161-168°C; purity: 94%; IR (ν/cm^{-1}) ν (C=O, conjugated) : 1599, ν (OH) : 3303

2-(6-(4-methoxystyryl)-2,4-dimethoxyphenyl)-7-fluoro-3-hydroxy-4*H*-chromen-4-one (**12**)

Yield: 80%; m.p. 228-230°C; purity: 98%; IR (ν/cm^{-1}) ν (C=O, conjugated) : 1606, ν (OH) : 3289

2-(6-(4-methoxystyryl)-2,4-dimethoxyphenyl)-6-chloro-3-hydroxy-4*H*-chromen-4-one (**13**)

Yield: 56%; m.p. 180-182°C; purity: 98%; IR (ν/cm^{-1}) ν (C=O, conjugated) : 1598, ν (OH) : 3314

2-(6-(4-methoxystyryl)-2,4-dimethoxyphenyl)-6-fluoro-3-hydroxy-4*H*-chromen-4-one (**14**)

Yield: 87%; m.p. 196-200°C; purity: 98%; IR (ν/cm^{-1}) ν (C=O, conjugated) : 1603, ν (OH) : 3328

3-hydroxy-2-(naphthalen-1-yl)-4*H*-chromen-4-one (**15**)

Yield: 32%; m.p. 202-204°C; purity: 98%; IR (ν/cm^{-1}) ν (C=O, conjugated) : 1602, ν (OH) : 3358

3-hydroxy-6-methoxy-2-(naphthalen-1-yl)-4*H*-chromen-4-one (**16**)

Yield: 31%; m.p. 220-226°C; purity: 96%; IR (ν/cm^{-1}) ν (C=O, conjugated) : 1605, ν (OH) : 3290

3-hydroxy-2-(2-methoxynaphthalen-1-yl)-4*H*-chromen-4-one (**17**)

Yield: 94%; m.p. 240-242°C; purity: 98%; IR (ν/cm^{-1}) ν (C=O, conjugated) : 1608, ν (OH) : 3278

2-(2,3-dimethoxynaphthalen-1-yl)-3-hydroxy-6-methoxy-4*H*-chromen-4-one (**18**)

Yield: 64%; m.p. 280-284°C; purity: 98%; IR (ν/cm^{-1}) ν (C=O, conjugated) : 1596, ν (OH) : 3331

3-hydroxy-2-(4-methoxynaphthalen-1-yl)-4*H*-chromen-4-one (**19**)

Yield: 79%; m.p. 230-232°C; purity: 98%; IR (ν/cm^{-1}) ν (C=O, conjugated) : 1617, ν (OH) : 3339

3-hydroxy-2-(naphthalen-2-yl)-4*H*-chromen-4-one (**20**)

Yield: 50%; m.p. 190-192°C; purity: 98%; IR (ν/cm^{-1}) ν (C=O, conjugated) : 1605, ν (OH) : 3251

3-hydroxy-6-methoxy-2-(naphthalen-2-yl)-4*H*-chromen-4-one (**21**)

Yield: 40%; m.p. 200-203°C; purity: 98%; IR (ν/cm^{-1}) ν (C=O, conjugated) : 1599, ν (OH) : 3320

2-(naphthalen-1-yl)-4*H*-chromen-4-one (**22**)

Yield: 84%; m.p. 117-122°C; purity: 98%; IR (ν/cm^{-1}) ν (C=O, conjugated) : 1651, ν (CH, sp^2) : 3052

6-methoxy-2-(naphthalen-1-yl)-4*H*-chromen-4-one (**23**)

Yield: 39%; m.p. 108-112°C; purity: 98%; IR (ν/cm^{-1}) ν (C=O, conjugated) : 1640, ν (CH, sp^2) : 3052

5-methoxy-2-(naphthalen-1-yl)-4*H*-chromen-4-one (**24**)

Yield: 50%; m.p. 202-206°C; purity: 96%; IR (ν/cm^{-1}) ν (C=O, conjugated) : 1641, ν (CH, sp^2) : 3049

6,7-dimethoxy-2-(naphthalen-1-yl)-4*H*-chromen-4-one (25)

Yield: 45%; m.p. 170-176°C; purity: 98%; IR (ν/cm^{-1}) ν (C=O, conjugated) : 1629, ν (CH, sp^2) : 3004

7-methoxy-2-(naphthalen-1-yl)-4*H*-chromen-4-one (26)

Yield: 10%; m.p. 102-106°C; purity: 98%; IR (ν/cm^{-1}) ν (C=O, conjugated) : 1639, ν (CH, sp^2) : 3057

2-(naphthalen-2-yl)-4*H*-chromen-4-one (27)

Yield: 24%; m.p. 158°C; purity: 96%; IR (ν/cm^{-1}) ν (C=O, conjugated) : 1622, ν (CH, sp^2) : 3054

6-methoxy-2-(naphthalen-2-yl)-4*H*-chromen-4-one (28)

Yield: 70%; m.p. 210-214°C; purity: 97%; IR (ν/cm^{-1}) ν (C=O, conjugated) : 3057, ν (CH, sp^2) : 1635

2-(2-methoxynaphthalen-1-yl)-4*H*-chromen-4-one (29)

Yield: 81%; m.p. 200-202°C; purity: 98%; IR (ν/cm^{-1}) ν (C=O, conjugated) : 3052, ν (CH, sp^2) : 1642

6-methoxy-2-(2-methoxynaphthalen-1-yl)-4*H*-chromen-4-one (30)

Yield: 44%; m.p. 187-189°C; purity: 98%; IR (ν/cm^{-1}) ν (C=O, conjugated) : 1637, ν (CH, sp^2) : 3067

5-methoxy-2-(2-methoxynaphthalen-1-yl)-4*H*-chromen-4-one (31)

Yield: 85%; m.p. 74-78°C; purity: 98%; IR (ν/cm^{-1}) ν (C=O, conjugated) : 1642, ν (CH, sp^2) : 3060

6,7-dimethoxy-2-(2-methoxynaphthalen-1-yl)-4*H*-chromen-4-one (32)

Yield: 22%; m.p. 226-230°C; purity: 98%; IR (ν/cm^{-1}) ν (C=O, conjugated) : 1622, ν (CH, sp^2) : 3067

2-(4-methoxynaphthalen-1-yl)-4*H*-chromen-4-one (33)

Yield: 59%; m.p. 175-180°C; purity: 97%; IR (ν/cm^{-1}) ν (C=O, conjugated) : 1649, ν (CH, sp^2) : 3065

5,7-dimethoxy-2-(4-methoxynaphthalen-1-yl)-4*H*-chromen-4-one (34)

Yield: 98%; m.p. 202-208°C; purity: 97%; IR (ν/cm^{-1}) ν (C=O, conjugated) : 1641, ν (CH, sp^2) : 3074

7-methoxy-2-(4-methoxynaphthalen-1-yl)-4*H*-chromen-4-one (35)

Yield: 22%; m.p. 184-188°C; purity: 98%; IR (ν/cm^{-1}) ν (C=O, conjugated) : 1637, ν (CH, sp^2) : 3084

2-(2,3-dimethoxynaphthalen-1-yl)-7-methoxy-4*H*-chromen-4-one (36)

Yield: 95%; m.p. 154-160°C; purity: 95%; IR (ν/cm^{-1}) ν (C=O, conjugated) : 1640, ν (CH, sp²) : 3059

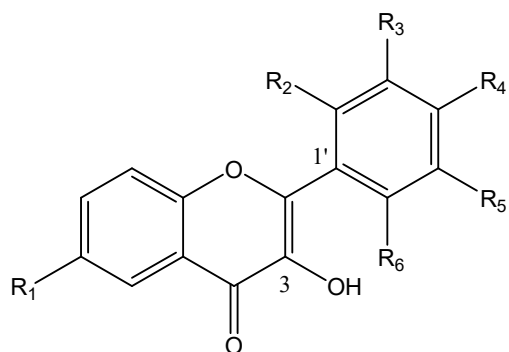
Supp. Table 1. A comparison of the pGI₅₀ values obtained from the clonogenic long-term survival assay with the values predicted using the CoMFA model, and their residual values. * denotes the derivatives contained in the test set.

derivatives	Experimental data (pGI ₅₀)	Predicted value (pGI ₅₀)	Residual (%)
1	1.39	1.46	-5.08
2	1.47	1.60	-8.18
3	2.35	2.28	2.89
4	1.43	1.36	4.99
5	1.78	1.82	-2.02
6	2.44	2.50	-2.32
7*	2.34	2.19	6.80
8	1.66	1.63	1.99
9	2.50	2.51	-0.49
10*	2.44	2.64	-8.01
11	2.58	2.57	0.29
12	2.51	2.50	0.40
13	2.54	2.54	0.11
14*	2.62	2.44	6.79
15	2.38	2.26	5.12
16	2.14	2.19	-2.39
17*	2.28	2.85	-24.96
18	2.12	2.15	-1.40
19	2.37	2.38	-0.67
20	2.62	2.61	0.24
21	2.51	2.56	-1.65
22*	2.54	2.06	18.69
23	2.62	2.40	8.29
24	2.14	2.17	-1.44
25	2.49	2.56	-2.82
26	2.59	2.59	0.13
27	1.52	1.57	-2.74
28	1.61	1.55	3.81
29*	2.39	2.70	-12.81
30	2.56	2.61	-2.23
31	3.31	3.31	-0.14
32*	2.42	2.81	-15.99
33	1.68	1.65	1.68
34	1.67	1.59	4.53
35	1.74	1.83	-5.15
36	2.40	2.38	0.89

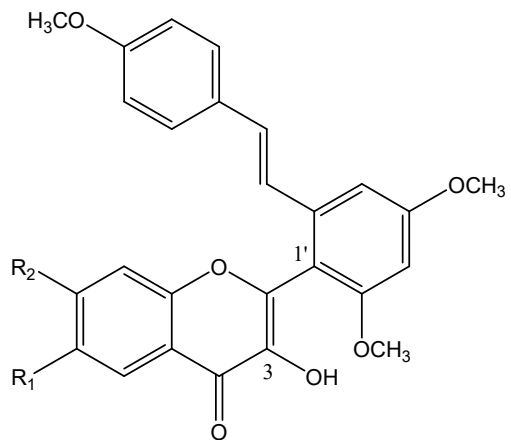
Supp. Table 2. A comparison of the pGI₅₀ values obtained from the clonogenic long-term survival assay with the values predicted using the CoMSIA model, and their residual values. * denotes the derivatives contained in the test set.

derivatives	Experimental data (pGI ₅₀)	Predicted value (pGI ₅₀)	Residual (%)
1	1.39	1.30	6.01
2	1.47	1.59	-7.80
3	2.35	2.19	6.56
4	1.43	1.40	2.21
5	1.78	1.75	1.70
6	2.44	2.55	-4.35
7*	2.34	1.84	21.57
8	1.66	1.55	6.76
9	2.50	2.56	-2.40
10*	2.44	2.84	-16.44
11	2.58	2.49	3.51
12	2.51	2.61	-3.92
13	2.54	2.49	2.17
14*	2.62	2.43	7.34
15	2.38	2.37	0.58
16	2.14	2.33	-8.82
17*	2.28	2.82	-23.92
18	2.12	2.17	-2.12
19	2.37	2.26	4.76
20	2.62	2.61	0.18
21	2.51	2.59	-3.14
22*	2.54	2.10	17.18
23	2.62	2.36	9.76
24	2.14	2.13	0.42
25	2.49	2.44	1.72
26	2.59	2.54	2.13
27	1.52	1.69	-10.62
28	1.61	1.70	-5.35
29*	2.39	2.70	-12.71
30	2.56	2.71	-5.99
31	3.31	3.24	2.11
32*	2.42	2.78	-14.91
33	1.68	1.70	-0.80
34	1.67	1.61	3.26
35	1.74	1.88	-7.77
36	2.40	2.34	2.82

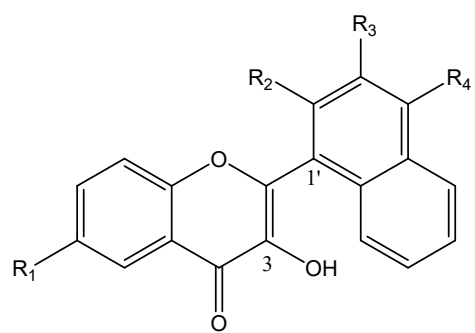
Suppl. Table 3. Structures of the 36 flavone derivatives.



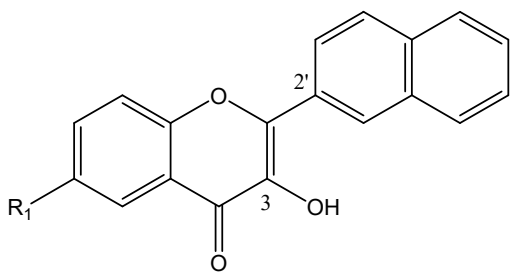
derivative	R ₁	R ₂	R ₃	R ₄	R ₅	R ₆
1	H	F	H	H	H	H
2	NO ₂	F	H	H	H	H
3	NO ₂	H	H	F	H	H
4	H	H	H	OCH ₃	H	H
5	H	OCH ₃	H	H	H	H
6	H	H	OCH ₃	OCH ₃	H	H
7	H	OCH ₃	H	OCH ₃	H	OCH ₃
8	H	OCH ₃	H	OCH ₃	H	H



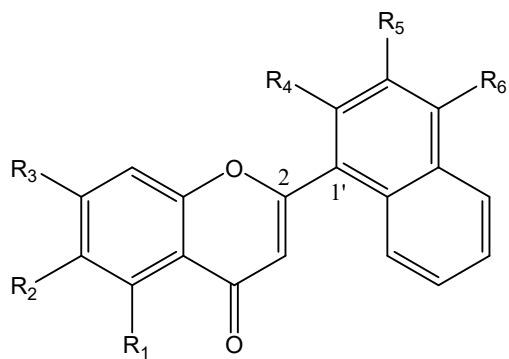
derivative	R ₁	R ₂
9	H	H
10	NO ₂	H
11	Br	H
12	H	F
13	Cl	H
14	F	H



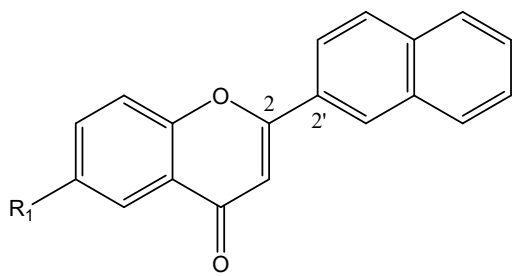
derivative	R ₁	R ₂	R ₃	R ₄
15	H	H	H	H
16	OCH ₃	H	H	H
17	H	OCH ₃	H	H
18	OCH ₃	OCH ₃	OCH ₃	H
19	H	H	H	OCH ₃



derivative	R_1
20	H
21	OCH ₃

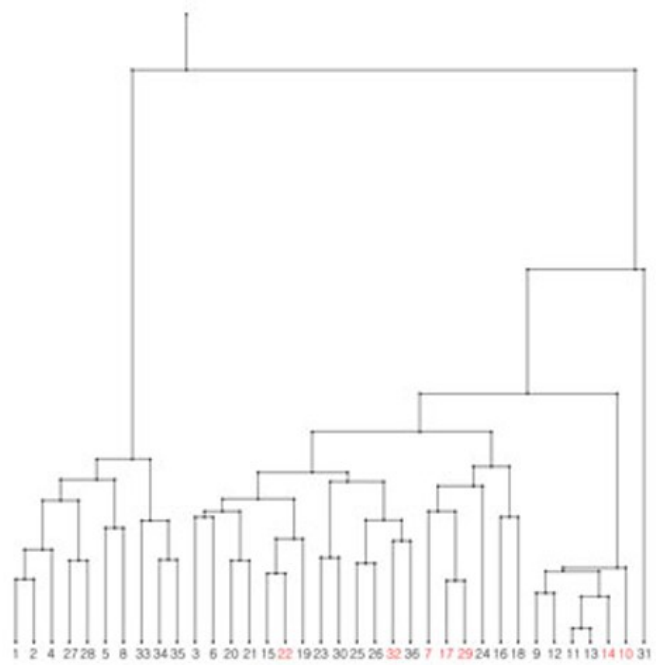


derivative	R ₁	R ₂	R ₃	R ₄	R ₅	R ₆
22	H	H	H	H	H	H
23	H	OCH ₃	H	H	H	H
24	OCH ₃	H	H	H	H	H
25	H	OCH ₃	OCH ₃	H	H	H
26	H	H	OCH ₃	H	H	H
29	H	H	H	OCH ₃	H	H
30	H	OCH ₃	H	OCH ₃	H	H
31	OCH ₃	H	H	OCH ₃	H	H
32	H	OCH ₃	OCH ₃	OCH ₃	H	H
33	H	H	H	H	H	OCH ₃
34	OCH ₃	H	OCH ₃	H	H	OCH ₃
35	H	H	OCH ₃	H	H	OCH ₃
36	H	H	OCH ₃	OCH ₃	OCH ₃	H

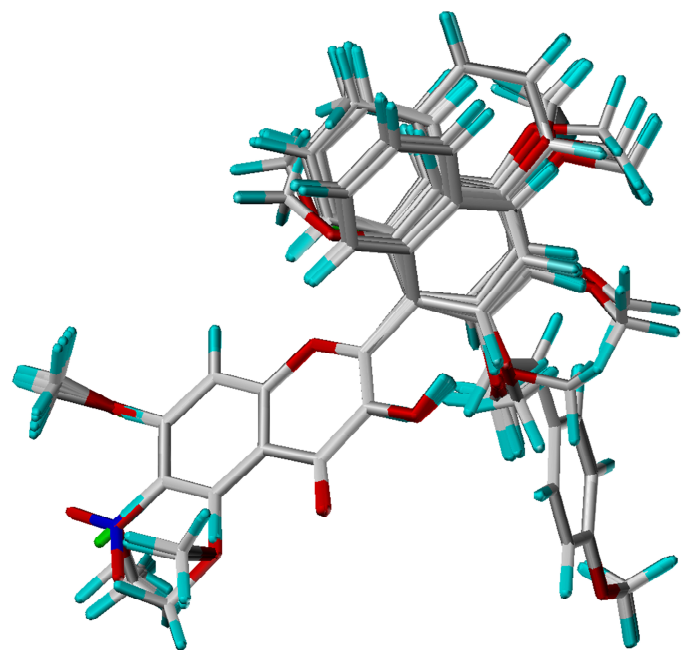


derivative	R ₁
27	H
28	OCH ₃

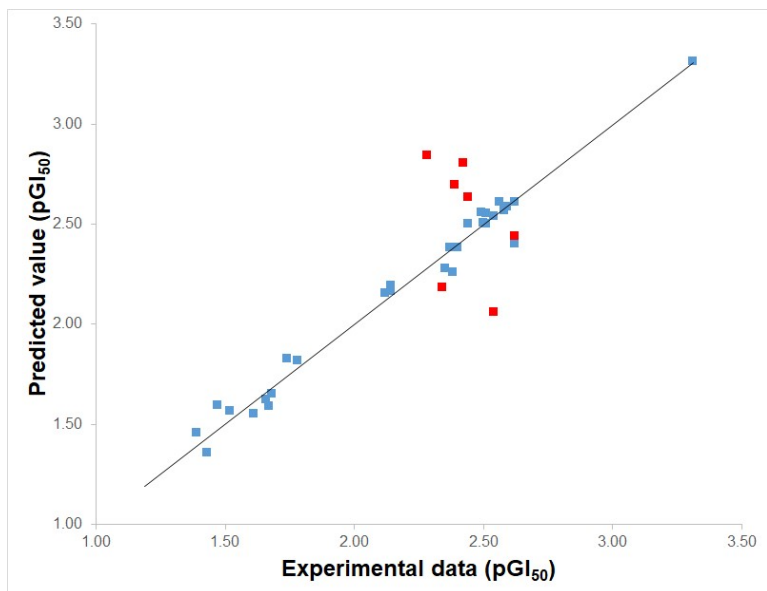
Suppl. Figure 1. Hierarchical clustering analysis used to select the test set.



Suppl. Figure 2. Alignments of 29 derivatives included in the training set.

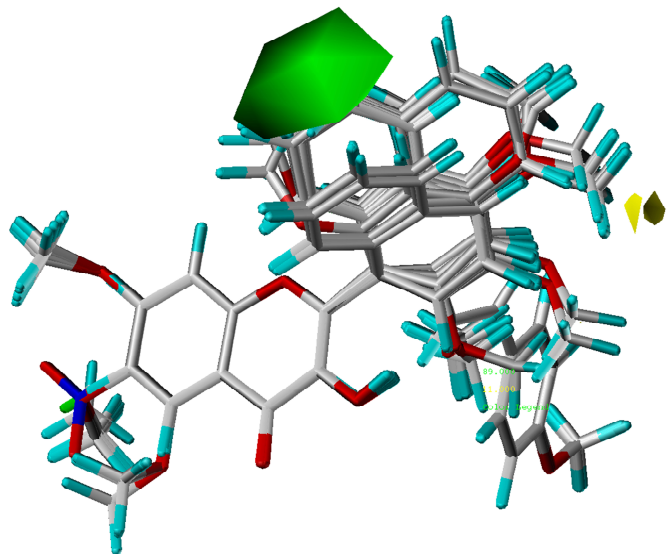


Suppl. Figure 3. A comparison of the experimental pGI₅₀ values obtained from the clonogenic long-term survival assay with the values predicted using the CoMFA model. The training set and the test set are denoted in blue and red squares, respectively.

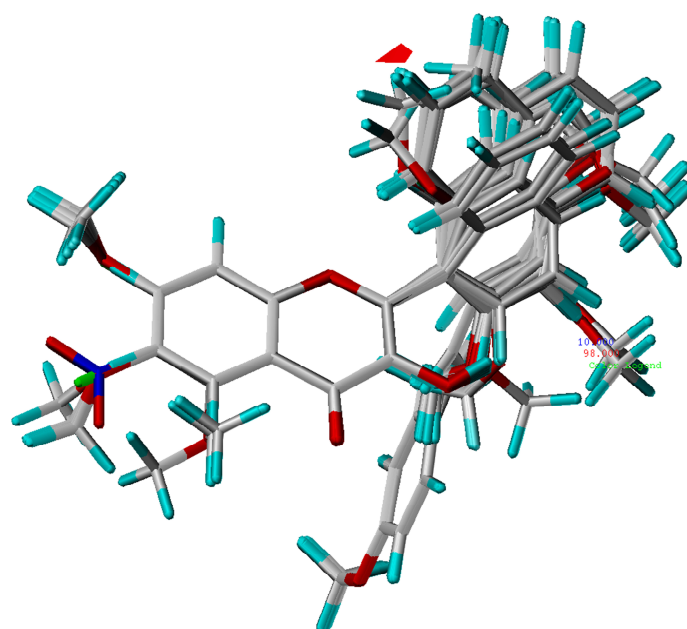


Suppl. Figure 4. (A) Contour maps of steric field descriptors generated by the CoMFA model. The bulk favoring (green) and disfavoring regions (yellow) occupied 92% and 8%, respectively. (B) Contour maps of electrostatic field descriptors. The electrostatic favoring (blue) and disfavoring regions (red) occupied 1% and 99% of the maps, respectively.

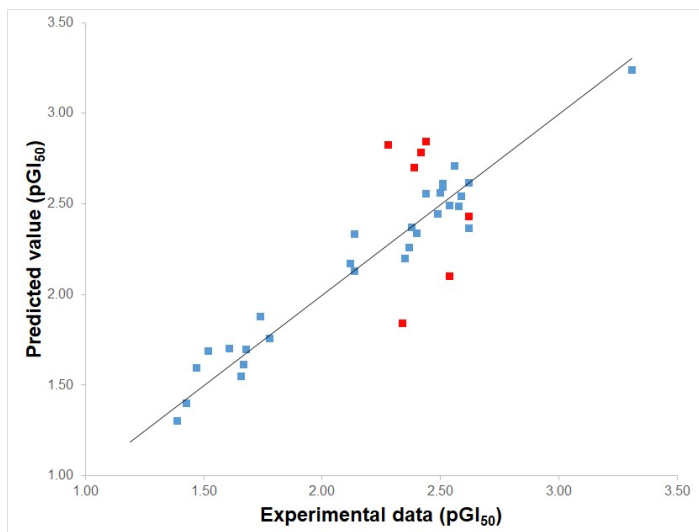
(A)



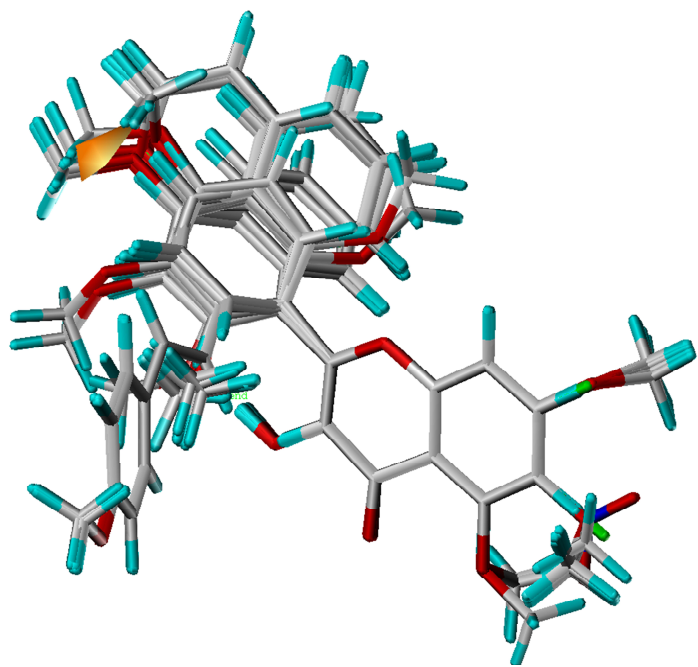
(B)



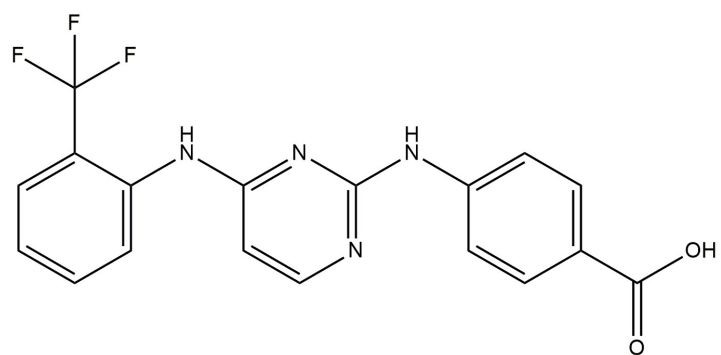
Suppl. Figure 5. A comparison of the experimental pGI₅₀ values obtained from the clonogenic long-term survival assay with the values predicted using the CoMSIA model. The training set and the test set are denoted in blue and red squares, respectively.



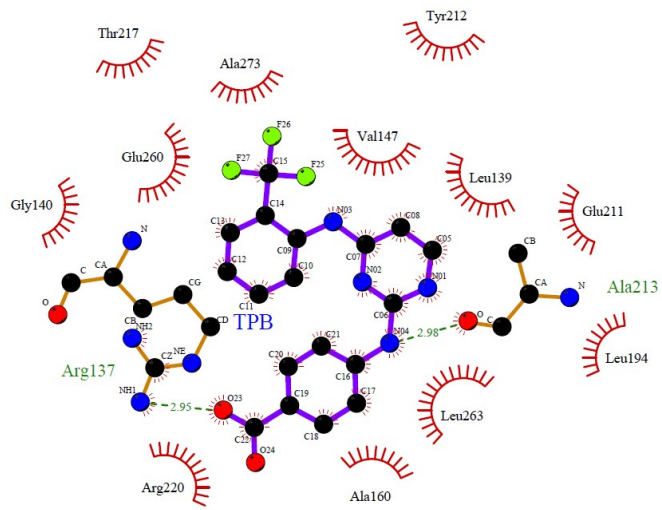
Suppl. Figure 6. Contour maps of hydrophobic field descriptors generated by the CoMSIA model. The hydrophobic favoring region (orange) occupied 95% and the disfavoring region (violet) 5%, of the contour map area.



Suppl. Figure 7. The structure of the ligand contained in AURKA deposited in the protein data bank as 3uod.pdb, 4-[(4-{[2-(trifluoromethyl)phenyl]amino}pyrimidin-2-yl)amino]benzoic acid.

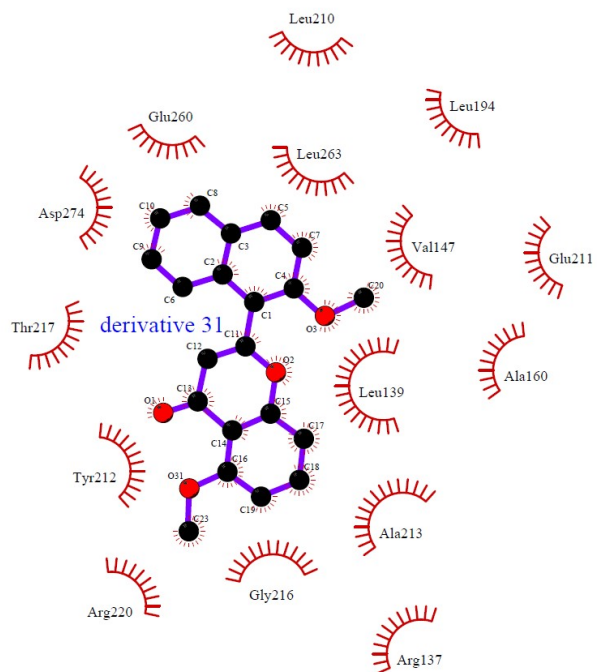


Suppl. Figure 8. Residues residing in the binding site of the AURKA – TPB complex obtained by the LigPlot analysis.



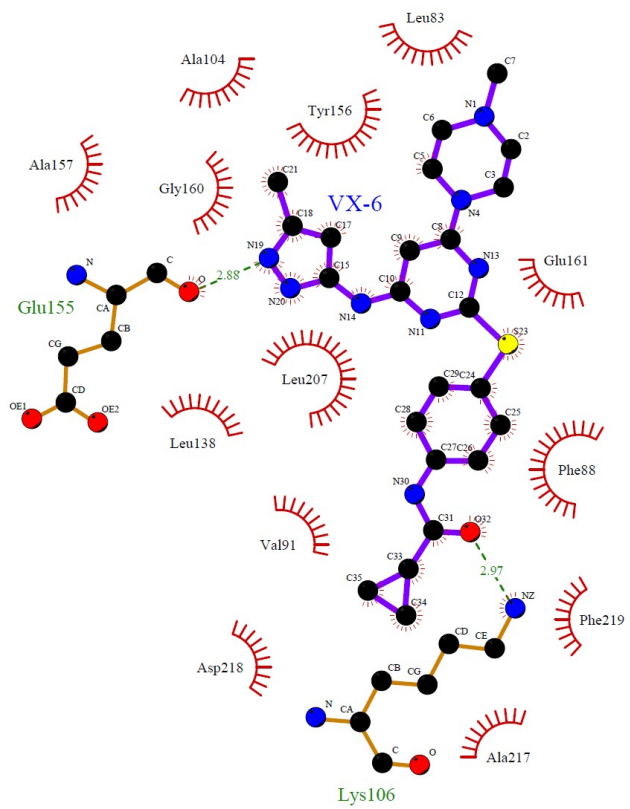
3uod

Suppl. Figure 9. Residues residing in the binding site of the AURKA – derivative **31** complex obtained by the LigPlot analysis.



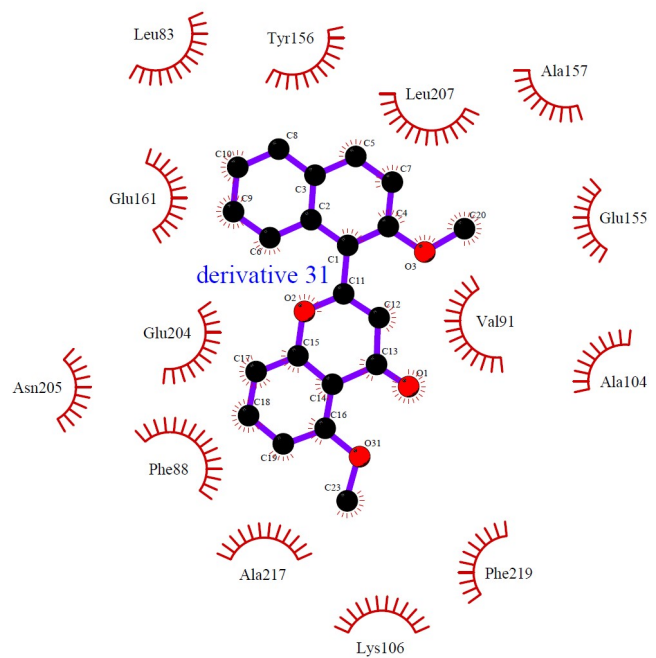
3uod

Suppl. Figure 10. Residues residing in the binding site of the AURKB – VX6 complex obtained by the LigPlot analysis.



4af3

Suppl. Figure 11. Residues residing in the binding site of the AURKB – derivative **31** complex obtained by the LigPlot analysis.



4af3

Suppl. Scheme 1. The synthetic procedure of 36 flavone derivatives [*Magn Reson Chem* **2017**, *55*, 359].

